

Simple quantum logic gate with quantum dot cavity QED systems

T. D. Ladd* and Y. Yamamoto

*Edward L. Ginzton Laboratory, Stanford University, Stanford, California 94305-4088, USA and**National Institute of Informatics, 2-1-2 Hitotsubashi, Chiyoda-ku, Tokyo 101-8430, Japan*

(Received 16 September 2011; published 6 December 2011)

We present a method to enact a deterministic, measurement-free, optically generated controlled-phase gate on two qubits defined by single electrons trapped in large-area quantum dots in a planar microcavity. This method is tolerant to optical quantum dot inhomogeneity, requires only a modest- Q planar cavity, employs only a single laser pulse, and allows the integration of many entangled qubits on one semiconductor chip. We present the gate in the contexts of both adiabatic evolution and geometric phases, and calculate the degradation of performance in the presence of both spontaneous emission and cavity loss.

DOI: [10.1103/PhysRevB.84.235307](https://doi.org/10.1103/PhysRevB.84.235307)

PACS number(s): 03.67.Lx, 37.10.Jk, 42.50.Pq, 85.35.Be

I. INTRODUCTION

Quantum computers offer potential speedups over classical computers for certain problems, but only if they are made sufficiently large, fast, and robust. Optically controlled quantum dots (QDs) are promising for this application due to their capabilities for ultrafast optical initialization, control, and measurement,^{1–5} as well as their strong interface to single photons.^{6,7} In the past decade, numerous proposals for entangling QDs with photons enhanced by optical cavities have emerged; for a few examples, see Refs. 8–12. However, most of these schemes fail when experimentally realistic values of the cavity quality factor Q and the vacuum Rabi splitting g are considered. Even for experimental parameters corresponding to the most heroic cavity quantum electrodynamics (QED) demonstrations, scaling these schemes may introduce unrealistic requirements for QD tuning and placement, or extremely challenging optical control sequences.

Here, we argue that an entangling logic gate between neighboring QD spins is possible in a planar microcavity using only a single pulse of laser light. Moreover, the gate we propose functions when the QDs have very different optical resonances, and without requiring the strong coupling regime of cavity QED. In conjunction with single-qubit initialization, control, and detection techniques, as well as the introduction of high-threshold, nearest-neighbor-only techniques for topological fault-tolerance in cluster states,¹³ this gate offers strong promise for a fast, scalable fault-tolerant quantum information processing system using QDs.^{14,15}

II. PRINCIPLE OF OPERATION

The single-pulse entangling gate may be understood as a consequence of the adiabatic theorem: A quantum system in an eigenstate remains in that eigenstate if its Hamiltonian does not change “too quickly.” For optical control, “too quickly” means that the duration of the optical pulse should be longer than the inverse of the optical detuning, which may easily be large enough to keep the adiabatic condition even with picosecond pulses. In large-area QDs, this ultrafast control is enabled by the large, mesoscopically enhanced oscillator strength of an exciton,^{16–18} which is enhanced by a factor of $(a/a_B^*)^2$ in comparison to that of an atom, where a is the QD radius and a_B^* is the effective Bohr radius.¹⁶

As shown in Fig. 1(a), a single spin in a QD has two Zeeman-split ground states (either an electron spin-1/2 or the $J = \pm 3/2$ states of a trapped hole). However, circularly polarized light connects only one of these levels, which we notate $|1\rangle_A$, to an optically excited trion state, which we notate $|e\rangle_A$. The other ground state, labeled $|0\rangle_A$ and with energy $-\hbar\omega_A$, is “dark,” and so is unaffected by the pulse. Neglecting the possibility of a cavity for the time being (and so with $\delta = 0$), when an optical pulse of amplitude $\Omega_A(t)$ is introduced with detuning Δ_A , the semiclassical Hamiltonian in the rotating reference frame of the optical pulse for qubit A changes as

$$H_A(t) = -\omega_A |0\rangle\langle 0|_A + \Delta_A |e\rangle\langle e|_A + \Omega_A(t) |e\rangle\langle 1|_A + \Omega_A^*(t) |1\rangle\langle e|_A. \quad (1)$$

The adiabatic theorem tells us that a system beginning in state $|1\rangle_A$ remains in state $|1\rangle_A$; however, this eigenstate is dynamically “dressed” by the field pulse into a state with reduced energy in comparison to the bare ground state. The resulting phase shift of this state—the ac-Stark shift—with respect to the dark state accomplishes a single-qubit rotation^{1–5} by an angle θ_A . The total angle θ_A accomplished over the duration of the pulse is $\theta_A = (\Delta_A/2) \int_{-\infty}^{\infty} [\sqrt{1 + 4\Omega_A^2(t)/\Delta_A^2} - 1] dt$. The data in Fig. 1(b) of Ref. 5 is well described by this equation, indicating adiabatic evolution.

To move to a two-qubit gate, we now add a second qubit and an optical cavity. The optical laser pulse couples to cavity modes indexed by μ ; each mode μ is detuned from the laser by δ_μ and annihilated by a_μ . The part of the pulse coupling to mode μ has (semiclassical) envelope $F_\mu(t)$ and coupling rate χ_μ , so the Hamiltonian for the optical pulse and the empty cavity is

$$H_{\text{optical}}(t) = \sum_{\mu} \delta_{\mu} a_{\mu}^{\dagger} a_{\mu} + \chi_{\mu} F_{\mu}(t) a_{\mu}^{\dagger} + \chi_{\mu}^{*} F_{\mu}^{*}(t) a_{\mu}. \quad (2)$$

Adding optical loss from cavity mode μ at rate κ_{μ} , an empty cavity would evolve by this Hamiltonian with state $[\prod_{\mu} D_{\mu}[\alpha_{\mu}(t)]] |\text{vac}\rangle$, for displacement operator $D_{\mu}[\alpha_{\mu}(t)] = \exp[\alpha_{\mu}(t) a_{\mu}^{\dagger} - \alpha_{\mu}(t) a_{\mu}]$ and

$$\alpha_{\mu}(t) = -i \int_0^t d\tau F_{\mu}(\tau) \exp\left[(\tau - t) \left(i\delta_{\mu} + \frac{\kappa_{\mu}}{2}\right)\right].$$

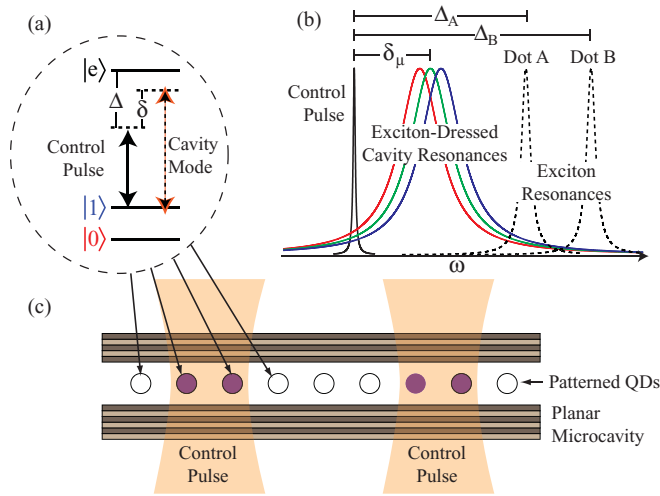


FIG. 1. (Color online) System schematic. (a) The energy levels of the quantum dot; level spin-ground-state $|1\rangle$ is coupled to trion state $|e\rangle$ by a cavity mode and control pulse. (b) The cavity, pulse, and dot spectra; the pulse is red-detuned from the cavity, and the dot's exciton resonances are blue-detuned. The cavity response is itself shifted by the presence of excitonic transitions, which depend on the qubit states. (c) Optical pulses are focused to overlap two neighboring patterned quantum dots in the planar microcavity.

As a first step of our quantum treatment, we work in an interaction picture where these dynamics are removed; i.e., we move from a density matrix $\rho(t)$ in the rotating reference frame to $\tilde{\rho}(t)$ in a different reference frame with the definition $\rho(t) = \prod_{\mu} D_{\mu}[\alpha_{\mu}(t)]\tilde{\rho}(t)\prod_{\nu} D_{\nu}^{\dagger}[\alpha_{\nu}(t)]$. This is a time-dependent basis change, and so it introduces time-dependent terms in our Hamiltonian; in particular, the cavity QED Hamiltonian becomes

$$H_{\text{CQED}} = \sum_{j=A,B} \sum_{\mu} g_{j\mu} |e\rangle\langle 1|_j a_{\mu} + \text{H.c.} \rightarrow \quad (3)$$

$$\tilde{H}_{\text{CQED}}(t) = \sum_{j=A,B} \sum_{\mu} g_{j\mu} |e\rangle\langle 1|_j [a_{\mu} + \alpha_{\mu}(t)] + \text{H.c.},$$

where H.c. is the Hermitian conjugate. If we now define $\Omega_j(t) = \sum_{\mu} g_{j\mu} \alpha_{\mu}(t)$, then in this reference frame we have a cavity QED system with an additional semiclassical driving term as already introduced in Eq. (1), so the full Hamiltonian is $\tilde{H}(t) = \sum_{\mu} \delta_{\mu} a_{\mu}^{\dagger} a_{\mu} + \sum_{j=A,B} H_j(t) + \tilde{H}_{\text{CQED}}(t)$.

A. Perturbative description

As in the single-QD case, if each $\Omega_j(t)$ evolves slowly enough, the action of the pulse is only to cause a phase shift on the adiabatically maintained bright states of the system. We will use a perturbative approach in our discussion, although all numeric calculations use exact diagonalizations or simulations. To fourth order in perturbation theory, the energies of the four qubit states shift according to the Feynman-like diagrams of Fig. 2. A superposition of qubit states evolves via these energy shifts, as

$$|\psi(t)\rangle = \sum_{j,k=\{0,1\}} c_{jk}(0) \exp\left[-i \int_0^t \lambda_{jk}(\tau)\right] |\lambda_{jk}(t)\rangle, \quad (4)$$

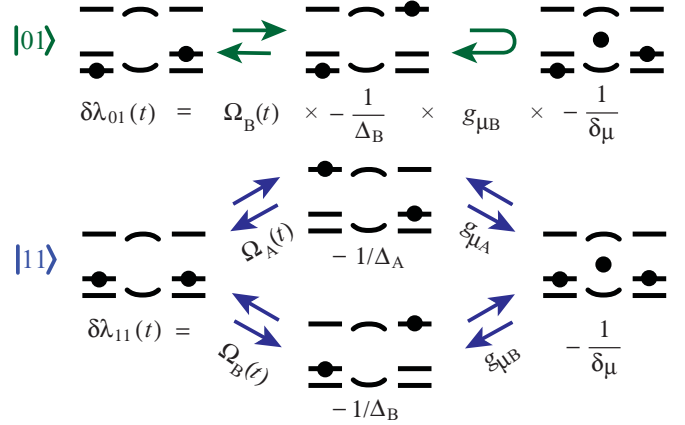


FIG. 2. (Color online) Diagrams for perturbative shifts of states $|01\rangle$ and $|11\rangle$. The stacks of three levels indicate the quantum dots, and a cavity photon is indicated by a dot in a center. The arrows indicate vertex terms, and the equations below indicate propagators. A complete (fourth-order) term is a product of each vertex and propagator.

where $|\lambda_{jk}(t)\rangle$ are the time-varying eigenstates of H which begin and end as separable qubit states $|\lambda_{jk}(0)\rangle = |\lambda_{jk}(\infty)\rangle = |j\rangle_A \otimes |k\rangle_B \otimes |\text{vac}\rangle$. An entangling gate results from the fact that the two-qubit bright state $|1\rangle_A \otimes |1\rangle_B \otimes |\text{vac}\rangle$ accrues less than twice the phase shift of either of the single-qubit bright states, such as $|1\rangle_A \otimes |0\rangle_B \otimes |\text{vac}\rangle$. The unitary evolution due to the pulse in this adiabatic, coherent approximation is $U = \exp(i\theta_A \sigma_A^z) \exp(i\theta_B \sigma_B^z) \exp(i\theta_{AB} \sigma_A^z \sigma_B^z)$, in terms of single-qubit Pauli matrices σ_j^z . The first two (commuting) terms are single-qubit phase shifts. These shifts may be large, as in demonstrated single-qubit rotations.¹⁻⁵ The entanglement results entirely from the smaller nonlinear phase θ_{AB} , which may be found in fourth order as

$$\theta_{AB} = - \int [\lambda_{11}(t) + \lambda_{00}(t) - \lambda_{01}(t) - \lambda_{10}(t)] dt$$

$$= 2 \text{Re} \left\{ \sum_{\mu} \int dt \frac{\Omega_A(t) \Omega_B^*(t) g_{A\mu} g_{B\mu}^*}{\Delta_A \Delta_B \delta_{\mu}} \right\} + O(g^6). \quad (5)$$

Note that there is no need for the QDs to be resonant with each other for this phase shift to occur, a critically important feature for inhomogeneous, self-assembled QDs.

B. Geometric description

This gate also has a geometric interpretation,^{19,20} rendering it similar to fast geometric phase gates enacted with trapped ions and their phonon modes.²¹ For this interpretation, we note that for qubits projected into states j and k , the field of mode μ is nearly classical with electric field amplitude proportional to $\alpha_{\mu}^{jk}(t) = \text{Tr}\{a_{\mu} \langle j|_A \langle k|_B \rho |j\rangle_A |k\rangle_B\}$. To second order, then, two of these amplitudes are

$$\alpha_{\mu}^{10}(t) = \alpha_{\mu}(t) + \sum_{\nu} \frac{g_{A\nu} g_{A\mu}^*}{\Delta_A \delta_{\mu}} \alpha_{\nu}(t) + O(g^4), \quad (6)$$

$$\alpha_{\mu}^{11}(t) = \alpha_{\mu}(t) + \sum_{j\nu} \frac{g_{j\nu} g_{j\mu}^*}{\Delta_j \delta_{\mu}} \alpha_{\nu}(t) + O(g^4). \quad (7)$$

We may interpret this by indicating that the cavity modes are shifted by the altered dispersive response of the cavity, depending on how many QDs are loading it. As the cavity field grows and then shrinks in time, a geometric phase accrues of size

$$\phi^{jk} = \int_{-\infty}^{\infty} dt \sum_{\mu} \text{Im} \{ \dot{\alpha}_{\mu}^{jk*}(t) \alpha_{\mu}^{jk}(t) \}, \quad (8)$$

i.e., the *area* enclosed by each phase-space path. In the limit of large detunings δ where $\text{Im} \{ \dot{\alpha}_{\mu}^{jk*}(t) \alpha_{\mu}^{jk}(t) \} \approx \delta_{\mu} |\alpha_{\mu}^{jk}(t)|^2$, this gives the same result, i.e., that $\phi^{11} + \phi^{00} - \phi^{01} - \phi^{10} = \theta_{AB}$, as given by Eq. (5). This geometric picture provides interesting perspective on the role of cavity loss. One may readily show in this picture that $\langle j|_A \langle k|_B \rho |j'\rangle_A |k'\rangle_B$ decays due to cavity loss as $\exp[-\int^t d\tau \sum_{\mu} \Gamma_{\mu}^{jk,j'k'}(\tau)]$, where

$$\Gamma_{\mu}^{jk,j'k'}(t) = \frac{\kappa_{\mu}}{2} |\alpha_{\mu}^{jk}(t) - \alpha_{\mu}^{j'k'}(t)|^2, \quad (9)$$

i.e., the *distance* between different paths. This decoherence occurs due to the ability of the environment to detect the qubit states from the light leaking from the cavity. A high detuning assures that state-dependent paths in phase space are very close to each other to minimize decoherence. If one wants to measure the qubit states using light leaked from the cavity, $\delta = 0$ is the best strategy;²² if one wants to protect the qubit states, a high value of δ allows the inherent quantum uncertainty of coherent states of light to hide the qubit states.

As a final note in this section, the present analysis may be readily generalized to more complex level structures. For example, if a full Λ system is employed with a small splitting between the ground states, a single pulse may still enact a gate, but now it will include qubit flip-flop terms, similar to two-laser cavity QED gates.⁸

III. FIDELITY ANALYSIS

Decoherence results from both cavity loss (at rate κ_{μ}) and spontaneous emission from the QDs (at rate γ). We may roughly estimate these effects with the following argument, in which we drop qubit subscripts for brevity. The dressed states of the system due to the pulse have a trion component with probability $(\Omega/\Delta)^2$ in first order, and they have a cavity photon with probability $(\Omega/\Delta)^2(g/\delta)^2$ in second order. Therefore, an off-diagonal term of the density matrix $\tilde{\rho}(t)$ decays at a combined exponent $\Gamma(t)$ of approximately

$$\Gamma(t) \approx x\gamma \frac{|\Omega|^2(t)}{\Delta^2} + y \sum_{\mu} \kappa_{\mu} \frac{\Omega^2(t) |g_{\mu}|^2}{\Delta^2 \delta_{\mu}^2}. \quad (10)$$

The unknowns x and y are in place to remind us that there are other, order-unity constants in place depending on the particular coherence studied. Regardless, optimal gate operations *must* work as a trade-off between the two decoherence terms. In the limit of large cavity-pulse detuning δ , taken as much larger than the cavity bandwidth (so $\delta_{\mu} \approx \delta$), the rate of growth of the nonlinear phase divided by the rate of decoherence $\Gamma^{-1}(t)\dot{\theta}_{AB}$ has a maximum with respect to δ at $\delta \propto \sqrt{\sum_{\nu} \kappa_{\nu} |g_{\nu}|^2 / \gamma}$. If we tune the laser in order to set δ at this value, and assure that $\int \Omega^2(t) dt$ is large enough that $\theta_{AB} = \pi/4$, then off-diagonal terms decay to

roughly $\exp[-\int \Gamma(t) dt] \approx \exp[-(\pi/2)\sqrt{xy/C}]$, where $C = 4 \sum_{\mu} |g_{\mu}|^2 / \gamma \kappa_{\mu}$ is the *cooperativity* of the QD/cavity system. The fidelity of the gate is then $\sim [1/2][1 + \exp(-1/\sqrt{C})]$. Note that QD inhomogeneity is not critical for determining the gate fidelity. The critical figure of merit, the cooperativity factor C , goes as the quality factor of the cavity Q divided by its mode volume V . A high-fidelity gate uses a laser detuned by \sqrt{C} cavity bandwidths from the cavity resonance; for a large-area QD in a semiconductor planar microcavity, $C \sim 100$ is reasonable, in which case the optimal detuning is approximately ten cavity linewidths from the central resonance.

The analysis so far has assumed the conditions allowing adiabatic evolution. For the present problem, in the case of detunings δ and Δ large in comparison to the cavity bandwidth and to Rabi frequencies $g_{j\mu}$, these conditions are held if $\dot{\Omega}_j(t) \sim \sum_{\mu} g_{j\mu} F_{\mu}(t) \ll \Delta_j^2$. Again assuming the amplitude of $F_{\mu}(t)$ is chosen large enough to create a controlled-Z gate ($\theta_{AB} = \pi/4$) with δ_{μ} at its optimum value, and assuming a Gaussian pulse shape $F_{\mu}(t) \propto (2\pi\sigma^2)^{-1/4} \exp(-t^2/4\sigma^2)$, this condition requires $\sigma \gg \sqrt{C} \kappa^2 / \Delta^2 \gamma$. Therefore, adiabaticity may always be obtained for long enough pulses and large enough values of Δ . Typical pulse lengths may be in the range of ten to hundreds of nanoseconds, with QD detunings Δ on the order of THz. This high speed is the key advantage of self-assembled QDs over similar gates enacted with trapped ions or superconducting qubits.

Evaluating the performance of the gate more rigorously than the above approximations requires a careful figure of merit, since as parameters are changed, the single-qubit phase shifts change much faster than the nonlinear phase shift. These single-qubit phase shifts can be eliminated by single-qubit π pulses, and therefore should not be considered to inhibit the fidelity of the gate; however, as they are not known *a priori*, evaluation of fidelity against an “ideal” gate with one particular choice of phase is inappropriate. Instead, we consider two qubits initialized into the unentangled superposition state $[|0\rangle_A + |1\rangle_A] \otimes [|0\rangle_B - |1\rangle_B] / 2$ and evaluate the entanglement concurrence. We then test our theory with a series of numeric approaches. In the first, we calculate the optimal value of $\Omega_j(t)$ using Eq. (5), assume the adiabatic theorem holds, and evaluate the phase shift and decay of each element of $\tilde{\rho}(t)$. This is accomplished via complete diagonalization of $\tilde{H}(t)$ at each time t , and tracking the evolution of diagonal terms of standard master equations for optical loss and spontaneous emission in the eigenvector basis. This procedure quickly estimates gate performance over a broad range of parameters, allowing a numeric search for the value of δ which maximizes the concurrence. The maximum concurrence resulting from this parameter search is shown in Fig. 3, which verifies that the figure of merit is indeed C . To test further, we perform detailed solutions of a complete master equation. No adiabatic or perturbative approximations are made; the time evolution of $\tilde{\rho}(t)$ is explicitly integrated using Runge-Kutta or semi-implicit extrapolation integration techniques. Again, only a single-cavity mode is assumed, but it may admit more than one photon. These simulations are slower, but verify the adiabatic theory for long enough pulse lengths.

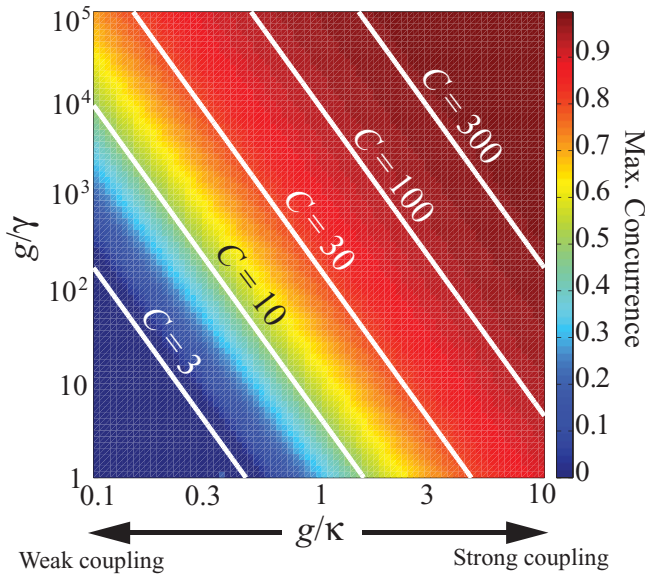


FIG. 3. (Color online) Concurrence of initially separable spins entangled by a gate with optimum δ , calculated numerically under the adiabatic approximation ($\sigma \rightarrow \infty$).

Realistically, it is unlikely that the adiabaticity of the system will limit the pulse length or the allowable detunings and homogeneity (Δ_A and Δ_B). As these detunings are increased, the amount of optical power required to complete a gate increases as well, and eventually additional decoherence sources not modeled here will arise. In InAs QDs and donor impurities in GaAs, such additional decoherence is seen in studies of single-qubit rotations, in many cases preventing high-fidelity pulses of large angles,⁴ but in other cases allowing them.⁵ The optimization of sample parameters to balance QD inhomogeneity and allowable optical power will be the critical hurdle for the successful demonstration of this gate in a semiconductor system.

IV. IMPLEMENTATION

We now address the type of small-mode-volume cavity to be used for this gate. Transmission line resonators in circuit cavity QED,²³ photonic crystal cavities,⁷ and whispering

gallery modes of microdisks²⁴ are possibilities, and if such cavities are critically coupled to waveguides and to other cavities to form complex “photonic molecules,” large-scale quantum computer architectures relying on this gate may be constructed.^{3,14} However, the large-scale integration of these cavity QED systems present a variety of challenges. A promising, simpler route for scalability, enabled by a large-area QD lattice, is integration with a planar microcavity sample, as shown in Fig. 1(c). The two-qubit gate would function by exciting a laser spot with the inherent cavity mode size $r_C = \lambda_0 / \sqrt{2\pi(1-R)}$, where λ_0 is the optical wavelength in vacuum and $R = \sqrt{R_1 R_2}$ is the effective reflectivity,²⁵ which overlaps two neighboring, site-controlled QDs in a two-dimensional array.²⁶ The cooperativity factor of a QD in a planar microcavity is not the same as that of a point dipole; instead, it depends on the size of the QD. The mode volume V may be estimated under the optimal condition that the angular distribution of the density of photon states of the cavity match the dipole emission lobe of the QD.¹⁶ In this case $4 \sum_{\mu} |g_{\mu}|^2 / \kappa_{\mu} / \gamma \approx Q \lambda_0^3 / [\pi^3 (a_B^*)^2 L]$, where L is the cavity length. This approximation is valid for QDs large in comparison to the optical wavelength in the semiconductor. High values of concurrence are expected to be possible with existing quality factors of planar microcavities²⁷ and site-controlled, large-area quantum QDs.²⁶

V. PROSPECTS

The key advantages of the present proposal are a tolerance to quantum dot inhomogeneity and compatibility with a relatively simple, microplanar cavity design. The potential parallelism of this two-qubit gate and the ability to array as many as 10^9 qubits on a single wafer may allow several possible architectures for fast and large-scale optically controlled quantum computers. One such architecture, recently developed and employing this gate concept, is detailed in Ref. 15.

ACKNOWLEDGMENTS

We acknowledge fruitful discussions with Bill Munro, Kae Nemoto, and Sebastien Louis. This work was supported by the National Science Foundation CCR-08 29694, NICT, and FIRST program of JSPS.

*Currently at HRL Laboratories, LLC, 3011 Malibu Canyon Rd., Malibu, CA 90265; tdladd@gmail.com

¹S. E. Economou, L. J. Sham, Y. W. Wu, and D. G. Steel, *Phys. Rev. B* **74**, 205415 (2006).

²C. E. Pryor and M. E. Flatté, *Appl. Phys. Lett.* **88**, 233108 (2006).

³S. M. Clark, K. M. C. Fu, T. D. Ladd, and Y. Yamamoto, *Phys. Rev. Lett.* **99**, 040501 (2007).

⁴J. Berezovsky, M. H. Mikkelsen, N. G. Stoltz, L. A. Coldren, and D. D. Awschalom, *Science* **320**, 349 (2008).

⁵D. Press, T. D. Ladd, B. Y. Zhang, and Y. Yamamoto, *Nature (London)* **456**, 218 (2008).

⁶J. P. Reithmaier *et al.*, *Nature (London)* **432**, 197 (2004).

⁷I. Fushman, D. Englund, A. Faraon, N. Stoltz, P. Petroff, and J. Vuckovic, *Science* **320**, 769 (2008).

⁸A. Imamoglu, D. Awschalom, G. Burkard, D. P. DiVincenzo, D. Loss, M. Shermin, and A. Small, *Phys. Rev. Lett.* **83**, 4204 (1999).

⁹L. M. Duan and H. J. Kimble, *Phys. Rev. Lett.* **92**, 127902 (2004).

¹⁰M. Feng, I. D’Amico, P. Zanardi, and F. Rossi, *Phys. Rev. A* **67**, 014306 (2003).

¹¹W. Yao, R.-B. Liu, and L. J. Sham, *Phys. Rev. Lett.* **95**, 030504 (2005).

¹²G. F. Quinteiro, J. Fernandez-Rossier, and C. Piermarocchi, *Phys. Rev. Lett.* **97**, 097401 (2006).

- ¹³R. Raussendorf and J. Harrington, *Phys. Rev. Lett.* **98**, 190504 (2007).
- ¹⁴R. Van Meter, T. D. Ladd, A. G. Fowler, and Y. Yamamoto, *Int. J. Quantum Inf.* **8**, 295 (2010).
- ¹⁵N. C. Jones, R. Van Meter, A. G. Fowler, P. L. McMahon, J. Kim, T. D. Ladd, and Y. Yamamoto, e-print [arXiv:1010.5022](https://arxiv.org/abs/1010.5022).
- ¹⁶G. Bjork, S. Pau, J. Jacobson, and Y. Yamamoto, *Phys. Rev. B* **50**, 17336 (1994).
- ¹⁷N. H. Bonadeo, G. Chen, D. Gammon, and D. G. Steel, *Phys. Status Solidi B* **221**, 5 (2000).
- ¹⁸J. R. Guest, T. H. Stievater, X. Q. Li, J. Cheng, D. G. Steel, D. Gammon, D. S. Katzer, D. Park, C. Ell, A. Thranhardt, G. Khitrova, and H. M. Gibbs, *Phys. Rev. B* **65**, 241310 (2002).
- ¹⁹S.-B. Zheng, *Phys. Rev. A* **70**, 052320 (2004).
- ²⁰T. P. Spiller, K. Nemoto, S. L. Braunstein, W. J. Munro, P. van Loock, and G. J. Milburn, *New J. Phys.* **8**, 30 (2006).
- ²¹J. J. García-Ripoll, P. Zoller, and J. I. Cirac, *Phys. Rev. A* **71**, 062309 (2005).
- ²²T. D. Ladd, P. van Loock, K. Nemoto, W. J. Munro, and Y. Yamamoto, *New J. Phys.* **8**, 184 (2006).
- ²³R. J. Schoelkopf and S. M. Girvin, *Nature (London)* **451**, 664 (2008).
- ²⁴E. Peter, P. Senellart, D. Martrou, A. Lemaître, J. Hours, J. M. Gérard, and J. Bloch, *Phys. Rev. Lett.* **95**, 067401 (2005).
- ²⁵G. Bjork, H. Heitmann, and Y. Yamamoto, *Phys. Rev. A* **47**, 4451 (1993).
- ²⁶C. Schneider *et al.*, *Appl. Phys. Lett.* **92**, 183101 (2008).
- ²⁷S. Reitzenstein *et al.*, *Appl. Phys. Lett.* **90**, 251109 (2007).